ACS Catalysis

Research Article

pubs.acs.org/acscatalysis

Roles of Acid Sites on Pt/H-ZSM5 Catalyst in Catalytic Oxidation of Diesel soot

Shuang Liu,[†] Xiaodong Wu,*[,‡] Duan Weng,*[,†] Min Li,[‡] and Rui Ran[†]

[†]State Key Laboratory of New Ceramics & Fine Processing and [‡]The Key Laboratory of Advanced Materials of Ministry of Education, School of Materials Science and Engineering, Tsinghua University, Beijing 100084, People's Republic of China

Supporting Information

ABSTRACT: Pt/H-ZSM5 and Pt/Al_2O_3 with similar surface Pt particle sizes and chemical states were prepared by incipient wetness impregnation as catalysts for soot oxidation. Pt/H-ZSM5 exhibits obviously higher activities in both O_2 and NO + O_2 than Pt/Al_2O_3. On the basis of the results obtained with in situ DRIFT and other structural and surface property characterizations, the high catalytic activity of Pt/H-ZSM5 is currently attributed to two main factors. First, the acidic H-ZSM5 support inhibits NO_2 adsorption on the catalyst, leading to a preferential adsorption of NO_2 on the surface of soot and providing more chances for NO_2−soot reactions. Second, the strong acid sites on the surface of Pt/H-ZSM5 can participate in the catalytic formation and decomposition of surface oxygenated complexes. Consequently, a high catalytic efficiency for soot oxidation is achieved on the Pt/H-ZSM5 catalyst.

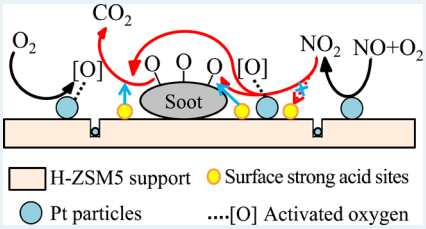

KEYWORDS: *Pt/H-ZSM5, soot oxidation, surface oxygenated complexes, surface acid sites, NO_2 preferential adsorption*

1. INTRODUCTION

Soot is produced as an unwelcome byproduct in many practical combustion systems. With internal combustion engines, particularly diesels, it can foul exhaust systems and present a severe environmental hazard when respired.[1] Trapping on diesel particulate filters (DPFs) followed by oxidation is an efficient way of elimination of soot particulate from diesel engine exhaust gas.[2,3] In order to avoid filter blocking, continuously regenerated trap (CRT) technology was further developed. In an advanced CRT system, NO_2 is generated by a platinum catalyst in the washcoat of the filter to promote soot oxidation at exhaust gas temperatures.[3−8] The corresponding reactions can be simply summarized as follows:

$$C + O_2 \rightarrow CO_2 \quad (1)$$

$$2NO + O_2 \xrightarrow{Pt} 2NO_2 \quad (2)$$

$$C + 2NO_2 \rightarrow CO_2 + 2NO \quad (3)$$

Thus, O_2- and NO_2-assisted soot oxidation mechanisms were proposed as eqs 1 and 3, respectively. In the latter case, NO_2 is generally suggested to initiate the creation of surface oxygenated complexes (SOCs), which are more reactive than the complexes that have already existed on soot. O_2 is then able to react with them and accelerate the total oxidation reaction.[9−12] Since NO_2 is a much more powerful oxidant than O_2, the NO_2-assisted mechanism (eq 3) was generally considered to be determinant for initiating and continuing soot oxidation.[3−8]

However, in our recent study, it was observed that the catalytic activity for NO oxidation did not exactly match the soot oxidation capacity on the sulfated Pt/Al_2O_3 catalyst.[8] On one hand, the acidic sulfates was observed to inhibit the NO_x adsorption on Al_2O_3, leading to a better adsorption and reaction between NO_x and soot. On the other hand, the sulfate species can promote the further decomposition of the SOCs. Thus, the sulfated Pt/Al_2O_3 with low NO oxidation activity exhibits superior activity for soot oxidation in NO + O_2. Nevertheless, there are several unsolved questions. First, although the influences of acid sites on SOCs decomposition have been proved, corresponding influences on the formation of these species have not yet been verified. Second, both Lewis and Brønsted acid sites may exist on an acidic material, but the specific mechanisms of how these acid sites affect the reactions still remain unclear. Finally, and the most important, sulfates over Pt/Al_2O_3 decompose at temperatures higher than 600 °C, making the application of the sulfated catalysts impractical.[13] On the other hand, Oi-Uchisawa et al.[5−7] studied Pt catalysts supported on various metal oxides and mixed oxides for soot oxidation and also found that acidic catalysts (such as Pt/Ta_2O_5 and Pt/Nb_2O_5) exhibit obviously better activities than Pt/Al_2O_3. However, they mainly focused on the sulfur resistance of these acidic catalysts under a SO_2-containing reaction atmosphere, instead of analyzing the reaction mechanism of acid sites. Thus, for an exploration the mechanism of the acid-promoted soot oxidation, a stable acidic support with plenty of acid sites (such as H-ZSM5) can be selected and studied in detail.

With a well-defined three-dimensional micropore structure, a capability for cation exchange, and capability for acid−base catalysis, H-ZSM5 has already become an applied catalyst for a

Received: September 16, 2014
Revised: December 24, 2014
Published: December 26, 2014

DOI: 10.1021/cs5018369
ACS Catal. 2015, 5, 909−919

variety of chemical processes.[14−19] Among them, Pt-loaded H-ZSM5 has been widely studied for hydroconversion, NO_x removal, and catalytic oxidation of volatile organic compounds,[16−19] while little attention has been paid to the potential of Pt/H-ZSM5 catalyst for soot oxidation so far. Villani et al.[3] investigated a series of Pt-loaded zeolites as catalysts for NO_x-assisted soot oxidation and observed that the zeolites were comparable to the more common alumina and titania supports. However, the catalysts they investigated have quite different Pt dispersions, which make a detailed comparison of different catalysts and exploration of the mechanism quite impossible. Therefore, a Pt/H-ZSM5 catalyst with the size and chemical state of surface Pt particles comparable with those of commercially applied Pt/Al_2O_3 should be studied, which may contribute to the discovery of the real potential of a new support without the disturbance of Pt structure effects.

In the present study, Pt/H-ZSM5 and Pt/Al_2O_3 with similar surface Pt particle sizes and chemical states were prepared. The catalysts were characterized by a series of structural and surface property measurements, and the roles of acid sites were proposed in a specific reaction mechanism over Pt/H-ZSM5 for soot oxidation.

2. EXPERIMENTAL SECTION

2.1. Materials. Pt (1 wt %) catalysts were prepared by incipient wetness impregnation of supports with appropriate amounts of an aqueous solution of $Pt(NO_3)_2$ (27.82 wt %, Heraeus). γ-Al_2O_3 (BASF with a BET surface of 150 m^2/g) and H-ZSM5 (NOVEL with a SiO_2/Al_2O_3 ratio of 17 and a BET surface of 270 m^2/g) were used as supports. The impregnated powders were submitted to drying at 110 °C overnight, and then the powders were calcined in static air at different temperatures (585 °C for Pt/Al_2O_3 and 500 °C for Pt/ZSM5) for 2 h to obtain catalysts with similar surface Pt particle sizes (PtAl and PtZSM5 for short). As a reference, a blank H-ZSM5 (ZSM5) was prepared by calcining the fresh H-ZSM5 in static air at 500 °C for 2 h.

Printex-U was used as model soot (diameter 25 nm, surface area 100 m^2/g, purchased from Degussa). Elemental analysis of Printex-U showed its carbonaceous nature with 92.0% C, 0.7% H, 3.5% O, 0.1% N, 0.2% S, and 3.5% other. The characterization of Printex-U was described in detail by Liu et al.[20] For further comparison, Printex-U was treated in a 500 ppm of NO_2/10% O_2/N_2 flow (500 mL/min) at 350 °C for 4 h to obtain the so-called "Nsoot". During this treatment, Printex-U was gradually oxidized in the $NO_2 + O_2$ mixture, resulting in a total mass loss of about 3−5%.[9−12] The residual soot was then collected and denoted as "Nsoot". Due to the reaction of surface R-NO_2 with O_2 during the SOCs formation, the existence of nitrogen groups on the surface of soot exposed in $NO_2 + O_2$ was excluded, as reported by Setiabudi et al.[12] Thus, the main difference between Nsoot and soot is the increased amount of SOCs (such as anhydride, carbonyl, and quinone species) on the former, as confirmed by the IR spectrum.[8]

2.2. Activity Measurements. The activities of the catalysts for soot oxidation were evaluated by temperature-programmed oxidation (soot-TPO) reactions in a fixed-bed reactor with the effluent gases monitored by an infrared spectrometer (Thermo Nicolet iS10). In the activity measurements, 10 mg of soot and 100 mg of sample were mixed with a spatula for 2 min in a reproducible way for "loose contact" conditions. To minimize the effect of hot spots, 110 mg of the soot−catalyst mixture was diluted with 300 mg of silica pellets, and then this mixture was sandwiched by quartz wool in a tubular quartz reactor. A gas mixture of either 1000 ppm of NO/10% O_2/N_2 (500 mL/min) or 10% O_2/N_2 (500 mL/min) with a gas hourly space velocity (GHSV) of 30000 h^{-1} was fed. The reactor temperature was then ramped to 600 °C at a heating rate of 10 °C/min. The T_{50} value (the temperature at which 50% of the soot was oxidized) was chosen to compare the catalytic activities of the samples. The downstream $CO_2/(CO_2 + CO)$ ratio during soot oxidation was defined as the selectivity to CO_2.

Meanwhile, to further investigate the intrinsic activity of the catalysts, the isothermal soot oxidation was performed at 300 °C in NO + O_2 and 400 °C in O_2, respectively, with the other reaction conditions were similar to those in the soot-TPO tests. At these temperatures, the soot conversion was low (<10%) and nearly constant over time. With the combination effects of a high space velocity and silica pellets, mass transfer limitation could be ignored, and no apparent temperature rise caused by soot oxidation was observed. Therefore, the reaction regime was mostly controlled by the chemical kinetics, instead of by mass and heat transfer.[2] The reaction rate (r_{soot}) and turnover frequency (TOF_{Pt}) were calculated on the basis of the isothermal soot oxidation reactions (see the Supporting Information) and were used to represent the intrinsic activity of the catalysts.

The NO temperature-programmed oxidation (NO-TPO) tests were carried out to evaluate the NO oxidation activity of different catalysts. They were performed in the same apparatus as that used in soot-TPO tests and also in a temperature-programmed oxidation (TPO) reaction apparatus at a heating rate of 10 °C/min. The inlet gas mixture was 1000 ppm of NO/10% O_2/N_2 with a total flow rate of 500 mL/min, while 100 mg of the catalyst was diluted with 300 mg of silica pellets in this reaction.

2.3. Characterizations. The powder X-ray diffraction (XRD) patterns were determined by a diffractometer (D8 ADVANCE, Bruker, Germany) employing Cu Kα radiation (λ = 0.15418 nm). The X-ray tube was operated at 40 kV and 30 mA. The X-ray diffractograms were recorded at 0.02° intervals in the range $20° \le 2\theta \le 80°$ with a scanning velocity of 4°/min.

Nitrogen adsorption−desorption isotherms at −196 °C were obtained with a JW-BK122F (Beijing JWGB, China) instrument. Prior to the analysis, the samples were degassed at 200 °C under vacuum for 2 h. The total surface area was obtained from the BET equation, and the external surface area and micropore volume were calculated from the *t*-plot method.

X-ray photoelectron spectra (XPS) were recorded on an ESCALAB 250 Xi system equipped with a monochromated Al Kα (1486.6 eV) X-ray source. The binding energy of C 1s (284.8 eV) was used as an internal standard. The high-resolution Pt 4d spectra were fitted using the XPSPEAK program by curve fitting with a Gaussian/Lorentzian ratio of 80/20 after subtraction of the Shirley-type background.

Samples for HRTEM analysis were prepared by dispersing the powder on holey carbon film supported on 3 mm Cu grids. A JEOL 2011 transmission electron microscope with a point resolution of 0.19 nm was used in this work. The size distribution of the platinum crystallites was determined by measuring 300 particles for each sample, and the mean Pt particle size was also calculated from these data.

CO titration experiments were conducted in the same apparatus as that used in NO-TPO tests. Prior to the test, the catalysts were treated in 30% O_2/N_2 at room temperature for 1

DOI: 10.1021/cs5018369
ACS Catal. 2015, 5, 909−919

Table 1. Overview of the Structural Properties of the Catalysts

catalyst	Pt dispersion (%)[a]	av Pt particle size (nm)[a]	av surface Pt particle size (nm)[b]	S_{BET} (m^2/g)	S_{Ext} (m^2/g)[c]	micropore volume (cm^3/g)[c]
PtAl	25.0	4.4	4.6	133	133	0.02
PtZSM	40.5	2.7	4.4	258	86	0.10
ZSM5				270	90	0.11

[a]Obtained from the CO titration results. [b]Estimated from the HRTEM results. [c]Obtained from the nitrogen physisorption at −196 °C.

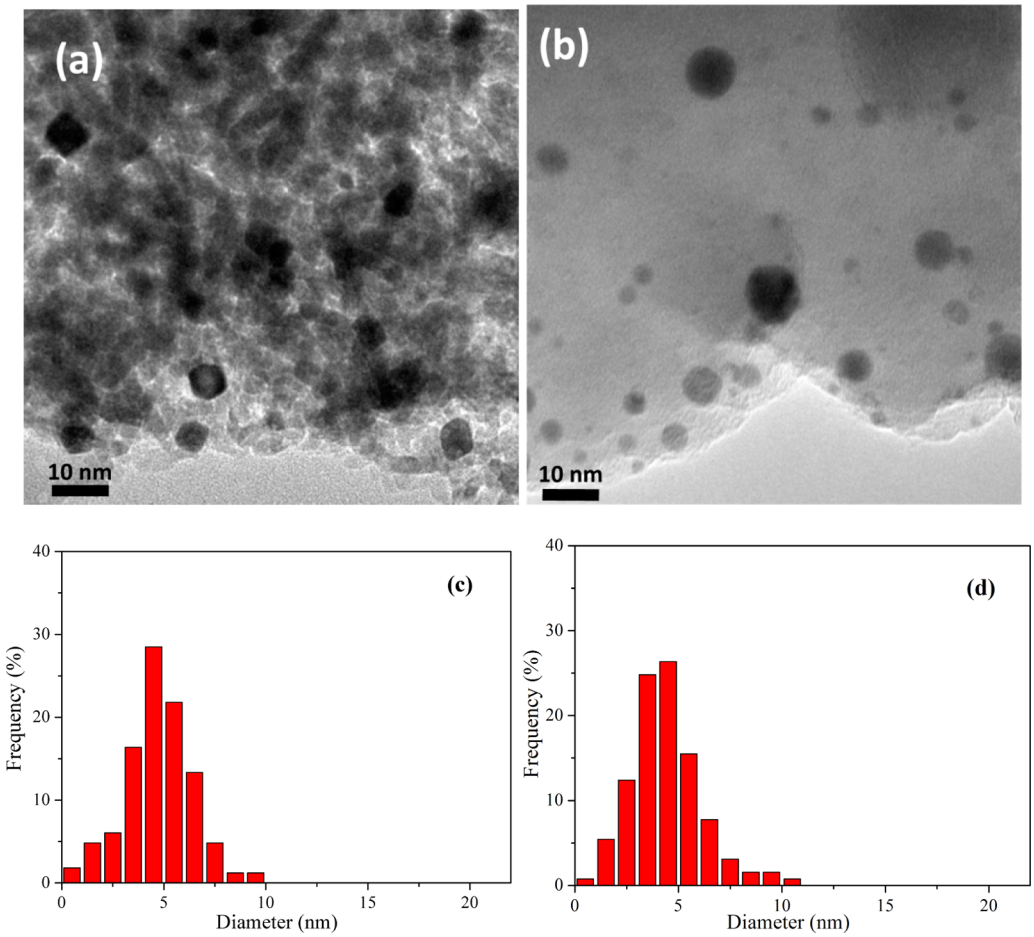

Figure 1. HRTEM images and size distributions of Pt particles on (a, c) PtAl and (b, d) PtZSM5.

h. The flow was then switched to N_2, and the reactor temperature was increased to 150 °C. Afterward, the flow was changed to 1% CO/N_2 and the outlet CO_2 concentration was analyzed and integrated. By assuming the reaction stoichiometry $CO + O\text{-}Pt_S \rightarrow CO_2 + Pt_S$, the number of Pt atoms and thereby the Pt dispersion could be obtained. The mean Pt particle size was determined from Pt dispersion data by assuming all of the Pt particles were spherical in shape.[8]

The NH_3 temperature-programmed desorption (NH_3-TPD) tests were performed in the same apparatus as that used in NO-TPO tests. Prior to the test, the sample powders were treated in nitrogen at 500 °C for 30 min for proper degassing. Then they were exposed in 1000 ppm of NH_3/N_2 at room temperature for 30 min and then flushed with N_2. Afterward, the NH_3 desorption profiles were obtained by ramping the reactor from room temperature to 600 °C at a heating rate of 10 °C/min under a nitrogen stream.

The NO_x temperature-programmed desorption (NO_x-TPD) tests were performed in the same apparatus as that used in NO-TPO tests. Prior to the test, the sample powders were exposed in 500 ppm of NO_2/10% O_2/N_2 (500 mL/min) at 350 °C for 30 min and then cooled to room temperature under the same atmosphere and flushed with N_2. Afterward, the NO and NO_2 desorption profiles were obtained by ramping the reactor from room temperature to 600 °C at a heating rate of 10 °C/min in a 10% O_2/N_2 stream.

The diffuse reflectance infrared Fourier transform spectra (DRIFTS) were recorded on a Nicolet 6700 FTIR spectrometer equipped with an MCT detector. A chamber blowing gas, N_2 (99.99% purity), was fixed at a flow rate of 100 mL/min. All of the samples (about 20 mg) were diluted with inert CaF_2 to obtain a feasible signal to noise ratio and were prepared with a 1:10:30 soot:catalyst:CaF_2 weight ratio (even if the sample contains only soot or catalyst, it would still be diluted with CaF_2 at the same weight ratio). After pretreatment in nitrogen (50 mL/min) at 500 °C for 30 min, the sample was then cooled to room temperature. Then the spectra were recorded from 100 to 550 °C at an interval of 50 °C in 500 ppm of NO_2/10% O_2/N_2. The spectra were then determined

DOI: 10.1021/cs5018369
ACS Catal. 2015, 5, 909−919

by accumulating 100 scans at a resolution of 4 cm^{-1} as a function of temperature at a heating rate of 10 °C/min.

3. RESULTS

3.1. Solid Properties. Figure S1 (Supporting Information) shows the XRD patterns of the catalysts. Only typical peaks of γ-Al_2O_3 and H-ZSM5 are observed in the diffraction patterns of the PtAl- and H-ZSM5-based catalysts, respectively. Diffraction peaks of metallic platinum or platinum oxide do not appear in the patterns, which is due to a good dispersion of Pt species on both of the high-surface-area supports (Table 1).

NO and soot catalytic oxidation over Pt catalysts is generally believed to depend strongly on the particle size of Pt.[3] As the Pt particles on PtAl and PtZSM5 are too small to be detected by XRD, high-resolution TEM images were obtained to characterize the Pt particle size on the catalyst surface. The corresponding Pt particle size distribution and the average platinum particle sizes are shown in Figure 1 and Table 1, respectively. It can be seen that PtAl and PtZSM5 exhibit similar average Pt particle size and distribution, indicating that the particle size effect of the precious metal can be ruled out in this work.

Since PtZSM5 has a porous microstructure with micropores of about 0.57 nm (Figure S2, Supporting Information), it is possible for Pt to partially enter these micropores and cause the catalyst to exhibit a bimodal distribution of Pt particle size (≤0.57 nm and around 4.4 nm). It is very difficult to observe the Pt particles with a size smaller than 1 nm directly by HRTEM images. Therefore, to quantitatively differentiate the surface and inner Pt distribution over PtZSM5, and exclude possible influence of the acidic support on CO adsorption, CO titration was employed to measure the Pt dispersions.[8]

It is worth noting that, since the kinetic diameters of CO (0.38 nm), O_2 (0.35 nm), and CO_2 (0.33 nm) are all smaller than the micropore size of PtZSM5 (0.57 nm), the CO titration results actually reflect the mean dispersion for Pt that exists both inside and outside of the zeolite micropores. As shown in Table 1, for the PtAl sample, the Pt particle size estimated by CO titration correlates well with that from HRTEM results. Meanwhile, a significantly higher Pt dispersion, and thereby a smaller average Pt particle size, is observed for PtZSM5, indicating the existence of small "inner" Pt particles in this catalyst. On the basis of these data, it was calculated that only 57−62% of the Pt is located on the surface of PtZSM5 (see the Supporting Information for the detailed calculation process), indicating that there is at least 38% of the Pt inside the micropores of PtZSM5 with particle sizes smaller than 0.57 nm.

In addition to the Pt particle size, the chemical states of the surface Pt particles may also influence the catalytic reaction. Figure 2 shows the XPS spectra of PtAl and PtZSM5. Due to the overlapping of the Pt 4f and the Al 2p peaks, the chemical states of Pt were determined using the Pt 4d peaks. It is clear that the Pt particles exist mainly in the 2+ oxidation state (PtO) on both catalysts.[21] Moreover, by calculation of the area ratio of the Pt^{2+} $3d_{5/2}$ (317.2 eV) and Pt^0 $3d_{5/2}$ (315.4 eV) peaks, it was found that PtAl comprises 87% PtO and 13% Pt, while PtZSM5 comprises 88% PtO and 12% Pt on the catalyst surface. Therefore, it seems that the electron density of the large surface Pt particles was not obviously affected by the supports, and the influence of Pt chemical states can be excluded in this work.

3.2. Catalytic Activities for NO and Soot Oxidation. Since NO_2 is crucial for soot oxidation in the loose-contact mode, the oxidation of NO to NO_2 is an important step in soot catalytic oxidation in NO + O_2.[3−8] Figure 3 shows the evolution of the outlet NO_2 and NO_x (NO + NO_2) concentration during the NO-TPO measurements. It is observed that PtZSM5 produces a lower amount of NO_2 in comparison with PtAl, indicating a worse NO oxidation activity of this catalyst. It has been widely accepted that the large Pt particles are far more active than the small particles for NO oxidation, which is because the small Pt particles can be readily oxidized to inert PtO_x.[22,23] Therefore, the NO oxidation results agree with the CO titration results and prove the existence of some small Pt particles in PtZSM5. The H-ZSM5 support itself seems to have no ability for NO oxidation, demonstrating the important role of Pt species.

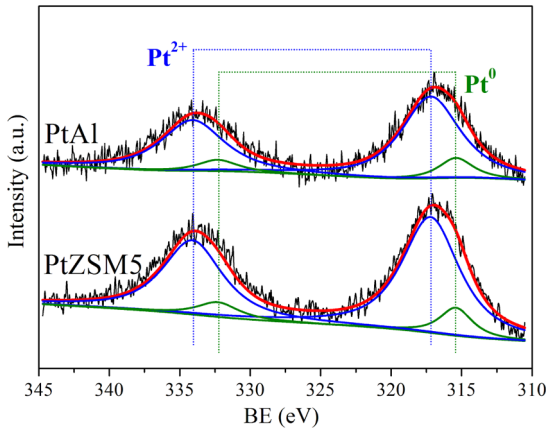

Figure 2. XPS spectra of PtAl and PtZSM5.

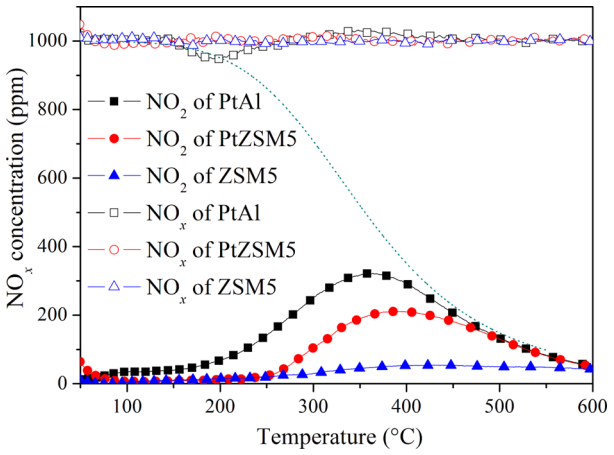

Figure 3. NO_2 and NO_x profiles during temperature-programmed oxidation of NO. Reactant gas: 1000 ppm of NO/10% O_2/N_2.

Furthermore, the concentration of NO_x (NO + NO_2) in the outlet gas was detected to observe possible adsorption of NO_x on the catalysts. Over PtZSM5, the total NO_x concentration remains almost constant with temperature. Meanwhile, for PtAl, the NO_x concentration decreases in the temperature range 150−280 °C due to the storage of NO_x on the catalyst, which is desorbed with a desorption peak centered at 350 °C. The results suggest a weaker NO_x storage capacity of PtZSM5 in comparison to tha tof PtAl, which will be confirmed by the NO_x-TPD results in section 3.4.

Figures S3−S5 (Supporting Information) show the TPO profiles of catalyzed and uncatalyzed soot oxidation under different conditions, while Figures S6 and S7 (Supporting

DOI: 10.1021/cs5018369
ACS Catal. 2015, 5, 909−919

Table 2. T_{50} (°C), Reaction Rate (r_{soot}, μmol s^{-1} g_{cat}^{-1}), and Turnover Frequency (TOF_{Pt}, 10^{-3} s^{-1}) of the Catalysts for Soot Oxidation under Different Conditions

	1000 ppm of NO/10% O_2/N_2			10% O_2/N_2					
	catalyst + soot			catalyst + soot			catalyst + Nsoot		
catalyst	T_{50}	r_{soot}[a]	TOF_{Pt}[b]	T_{50}	r_{soot}[c]	TOF_{Pt}[d]	T_{50}	r_{soot}[c]	TOF_{Pt}[d]
PtAl	460	0.206	1.61	546	0.149	1.16	545	0.152	1.21
PtZSM5	440	0.231	2.91−3.16	535	0.199	2.50−2.72	521	0.238	3.00−3.26
ZSM5	563	0.034		572	0.029		562	0.047	
uncatalyzed	570			575			573		

[a]Calculated on the basis of the amount of CO_x generated at 300 °C. [b]Calculated on the basis of the r_{soot} value at 300 °C and the CO titration results. [c]Calculated on the basis of the amount of CO_x generated at 400 °C. [d]Calculated on the basis of the r_{soot} value at 400 °C and the CO titration results.

Information) show the isothermal soot oxidation results. The T_{50}, reaction rate (r_{soot}), and turnover frequency (TOF_{Pt}) values are shown in Table 2. All of the platinum-containing catalysts yield a high CO_2 selectivity (>99%), while the ZSM5 sample and uncatalyzed reaction only exhibit CO_2 selectivity lower than 60% under all of the reaction conditions. It is interesting that, despite its lower NO oxidation activity, PtZSM5 exhibits an obviously higher activity than PtAl for soot oxidation in the presence of NO_x. Since the ZSM5 sample is almost inactive (it exhibits an activity similar to that of the uncatalyzed sample), the superior activity of PtZSM5 is most likely due to the synergistic effect of Pt and the H-ZSM5 support, rather than a simple combination of the catalytic oxidation over these two components. Also, this improvement should be effective enough that the negative influence of the weakened NO oxidation activity can be counteracted. In the absence of NO_x, the soot oxidation activities of platinum catalysts decrease dramatically. PtZSM5 is still the best catalyst among the three samples, but its advantage becomes less obvious in comparison with PtAl. These results indicate that the high activity of the platinum-containing catalysts, especially the PtZSM5 sample, is closely related with the NO_x utilization in the soot oxidation reaction.

In addition, it has been suggested that the further oxidation of the surface oxygenated complexes (SOCs) that formed by the NO_2 + soot reaction is an important step for soot oxidation.[3,8] In our previous study,[8] the NO_2-pretreated "Nsoot" was found to contain a larger amount of SOCs than Printex-U. Therefore, if one catalyst exhibits better catalytic performance in Nsoot oxidation than in soot oxidation, it can be deduced that the formation of SOCs on soot is limited in the latter reaction and the gap of the reaction rate between soot oxidation and Nsoot oxidation reflects the ability of catalyst for SOCs decomposition to a great extent. As shown in Figures S5 and S7 (Supporting Information) and Table 2, PtAl exhibits catalytic activity for Nsoot oxidation similar to that for soot oxidation, while the oxidation of Nsoot is accelerated over the H-ZSM5-based catalysts. These results indicate that, once the limitation of SOCs formation is minimized (as in the case of Nsoot oxidation), the H-ZSM5-based catalysts can efficiently accelerate the catalytic decomposition of the SOCs and thereby the total oxidation of soot. The poor SOCs decomposition ability of PtAl hinders it from presenting better activity. To further explore the specific mechanisms for the high activity of PtZSM5, a series of structural and in situ characterizations were also performed.

3.3. NH_3 Temperature-Programmed Desorption. Temperature-programmed desorption of NH_3 was carried out to determine the strength and amount of different acid sites. The NH_3-TPD profile of PtZSM5 shown in Figure 4 exhibits two desorption peaks in the temperature range below 500 °C, and

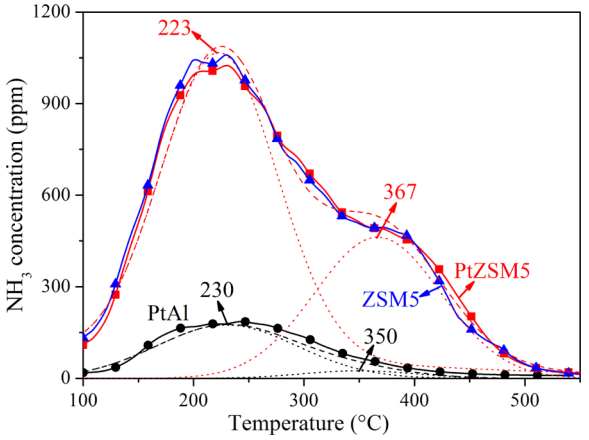

Figure 4. NH_3-TPD profiles of the catalysts.

the corresponding total NH_3 desorption amount is given in Table 3. The low-temperature desorption peak (maximum at about 230 °C) is due to weakly adsorbed NH_3, and the high-temperature desorption peak (maximum at about 360 °C) is caused by NH_3 desorption from strong (Brønsted and Lewis) acid sites.[14,15] The ZSM5 sample exhibits a desorption profile similar to that of the supported catalyst. The profiles were deconvoluted into two Gaussian functions associated with desorption at low and high temperatures, respectively. The amount of NH_3 adsorption over strong acid sites was calculated to be 339 and 16 μmol g_{cat}^{-1} for PtZSM5 and PtAl, respectively, indicating the richness of strong acid sites on the former catalyst.

Table 3. Amount of Acid Sites of the Catalysts

catalyst	total NH_3 desorption (mmol g_{cat}^{-1})[a]	total NH_3 desorption over strong acid sites (μmol g_{cat}^{-1})[b]	surface NH_3 desorption (mmol g_{cat}^{-1})[c]	surface NH_3 desorption over strong acid sites (μmol g_{cat}^{-1})
PtAl	0.16	16	0.14	14
PtZSM	1.02	339	0.34	113
ZSM5	1.04	330	0.34	110

[a]Calculated from the NH_3 desorbed in NH_3-TPD. [b]Calculated from the high-temperature NH_3 desorption in NH_3-TPD. [c]Calculated from the total NH_3 desorption considering the external surface area of the catalysts. [d]Obtained from the total NH_3 desorption over strong acid sites considering the external surface area of the catalysts.

DOI: 10.1021/cs5018369
ACS Catal. 2015, 5, 909−919

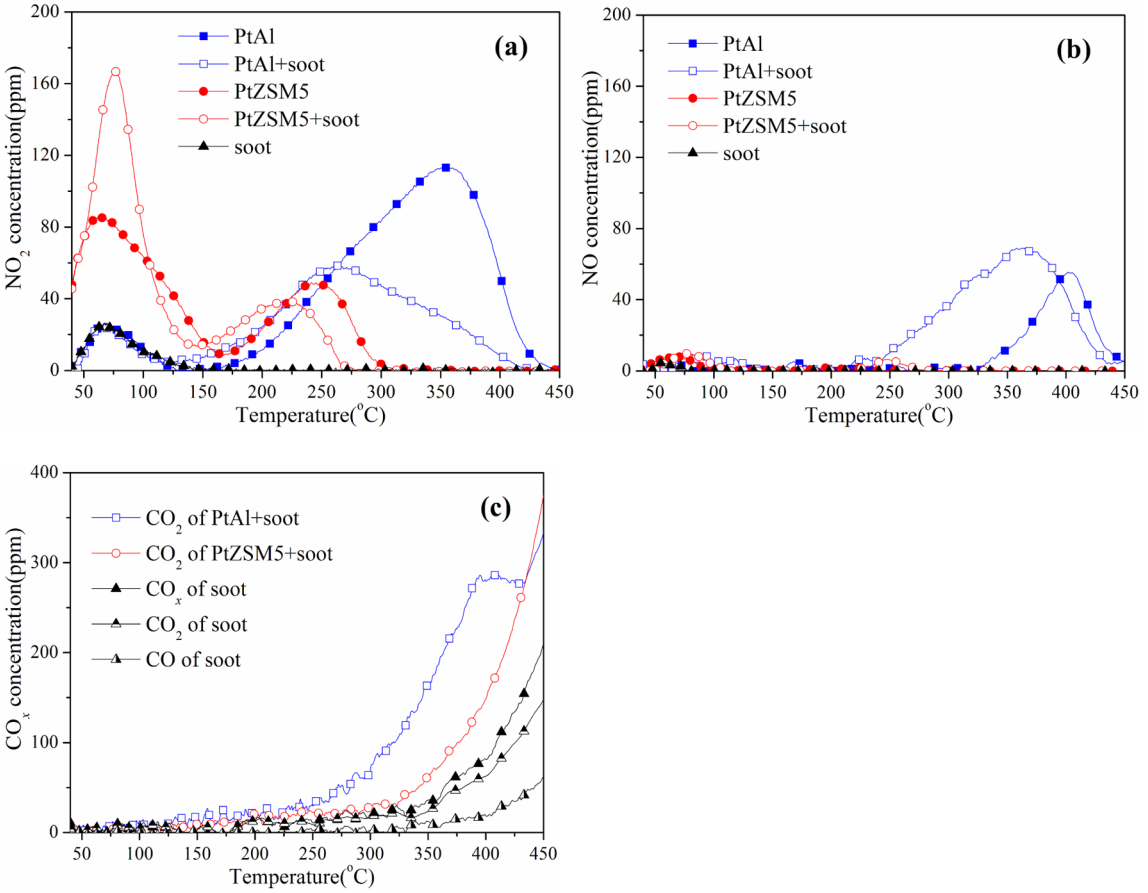

Figure 5. (a) NO_2 (b) NO, and (c) CO_x profiles in NO_x-TPD of the samples.

It should be kept in mind that the acidity characterized by NH_3-TPD corresponds to the acid sites both on the surface and inside the micropores of H-ZSM5 crystals. The latter acid sites are inaccessible for soot due to the much smaller sizes of the H-ZSM5 micropores (~0.57 nm) in comparison with those of soot particles (25 nm). Thus, before consideration of the role of acid sites for soot oxidation reactions, the amount of surface (accessible) and inner (inaccessible) acid sites should be specifically differentiated. Since the accessibility of acidic sites over ZSM5 has been proved to be linearly correlated with the external surface area,[24,25] the amount of NH_3 adsorbed on surface acid sites could be estimated by the equation $[NH_3]_{surf} = [NH_3]_{total} \times S_{Ext}/S_{BET}$. As shown in Table 3, the calculated amount of NH_3 adsorbed on surface acid sites of the catalyst is 0.34 and 0.14 mmol g_{cat}^{-1} for PtZSM5 and PtAl, respectively. This quantity turns out to be 113 μmol g_{PtZSM5}^{-1} and 14 μmol/g_{PtAl}^{-1} when only considering the strong acid sites on the catalyst surface. It can be seen that the amount of surface acid sites (especially the strong ones) for PtZSM5 is much larger than that for PtAl.

3.4. NO_x-TPD Results. NO_x-TPD tests were performed to evaluate the affinity toward NO_x species of different catalysts and the resulting influence on soot catalytic oxidation. Before the TPD process, the sample was pretreated in a NO_2-rich atmosphere (500 ppm of NO_2/10% O_2/N_2). It is seen in Figure 1 that the maximum NO_2 concentrations that are generated in the NO-TPO over PtAl and PtZSM5 are no more than 400 ppm. This means that the concentration of 500 ppm of NO_2 is beyond the possible amount of NO_2 produced during the reaction, which may eliminate the discrepancy in NO oxidation activities of different catalysts. Meanwhile, as indicated by Muckenhuber et al.,[10,11] soot can be readily oxidized under an atmosphere containing NO_2 and O_2. As shown in Figure S8 (Supporting Information), a small amount of CO_x formed on all the soot-containing samples during the NO_2-adsorption pretreatment. The soot consumption was calculated to be about 0.4%, 0.5%, and 0.5% for the soot, PtZSM5 + soot, and PtAl + soot, respectively. Therefore, this soot consumption can be excluded when analyzing the NO_x-TPD results.

As shown in Figure 5, a distinct NO_2 desorption peak and a weak NO desorption peak are observed over PtAl with a maximum at about 70 °C. This is due to either desorption of the physically adsorbed species or decomposition of nitrosyl, a weakly adsorbed species.[8,26] At temperatures higher than 150 °C, NO_2 exhibits a broad peak with a maximum at 350 °C, while NO has a maximum at 400 °C. The NO_2 desorptions at high temperatures are generally attributed to the decomposition of nitrate/nitrite couples, while NO may also come from thermodynamic issues related to NO_2 decomposition to NO + $^1/_2$ O_2.[27,28] With a larger BET surface area and micropore volume (Table 1), PtZSM5 exhibits physical adsorption of NO_x (decomposed at temperatures below 150 °C) much stronger than that of PtAl. However, the high surface acidity of PtZSM5 suppresses the formation and stability of nitrates/nitrites, and thus this catalyst releases much less NO_x than PtAl at temperatures higher than 150 °C.[8]

In addition to adsorption on the catalysts, the NO_x may also adsorb on carbon (soot). Zhu et al.[26] performed NO and NO +O_2 adsorption at 30 °C followed by a TPD process over

DOI: 10.1021/cs5018369
ACS Catal. 2015, 5, 909−919

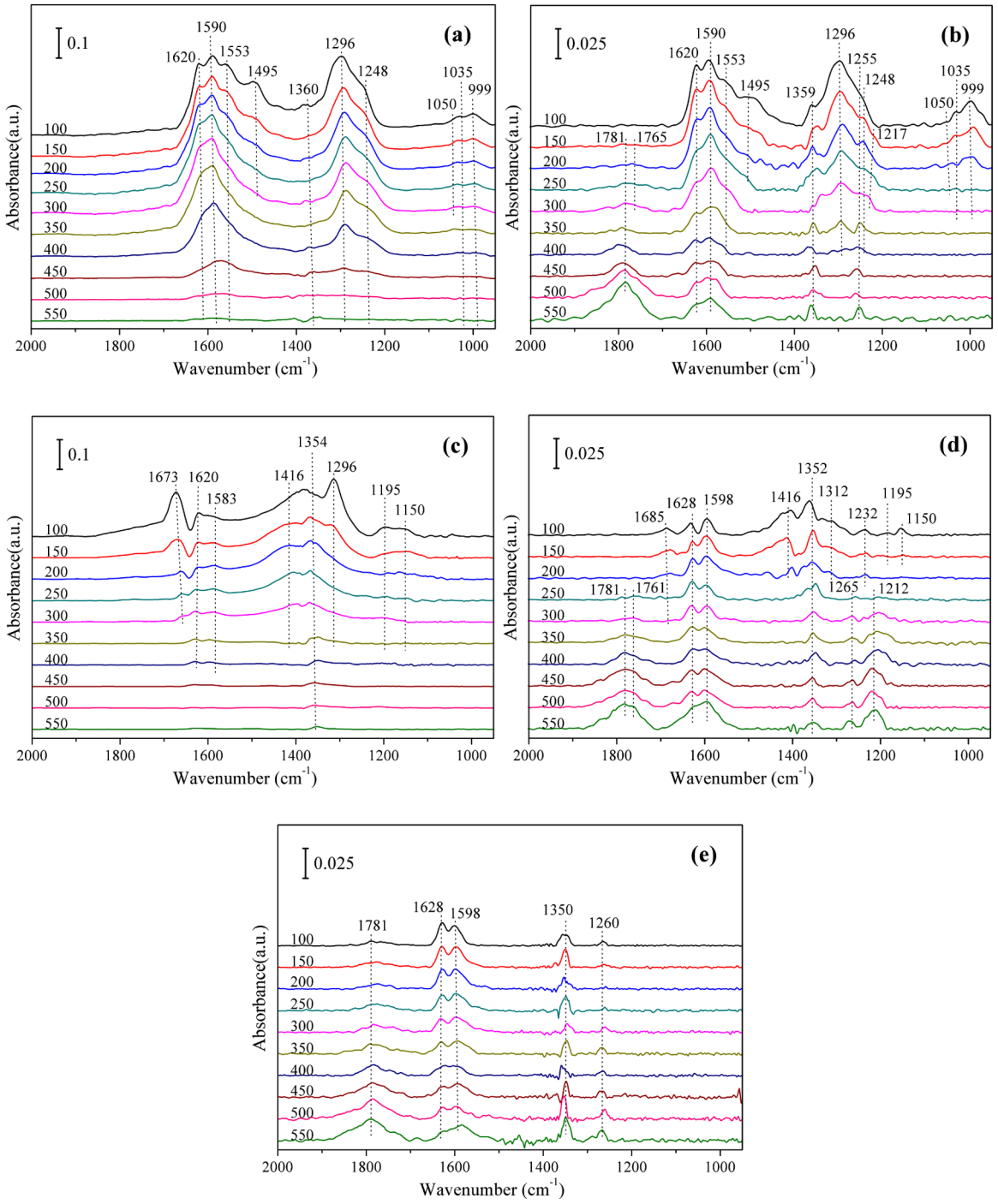

Figure 6. DRIFT spectra recorded over (a) PtAl, (b) PtAl + soot mixture, (c) PtZSM5, (d) PtZSM5 + soot mixture, and (e) soot exposed to 500 ppm of NO_2/10% O_2/N_2 at different temperatures.

activated coke. They attributed the different NO_x desorption profiles to various nitrosyl, nitrites, and nitrates that were stored on carbon. However, as the adsorption process was performed in NO_2 + O_2 at 350 °C in this study, the reaction between surface R-NO_2 and O_2 led to removal of the stable nitrate/nitrite species on soot.[12] Thus, only a low-temperature NO_2 desorption peak and a weak NO desorption peak at about 65 °C are observed on soot, which come from the decomposition of physically and/or weakly adsorbed species.

After the catalyst was mixed with soot, the PtAl + soot mixture showed a low-temperature NO_2 desorption peak quite similar to that of PtAl. However, this peak exhibited a remarkable increase in intensity over the PtZSM5 + soot mixture in comparison with PtZSM5. Considering the NO_x on pure soot desorbed mainly at low temperatures, it is reasonable to suggest that the soot in the PtZSM5 + soot mixture adsorbs much more NO_x than it does in PtAl + soot. The corresponding qualitative analysis of the NO_x-TPD results will be given in the Discussion.

The nitrate/nitrite-assisted soot oxidation mechanism has also been reported.[29−31] Such a reaction is observed during the NO_x-TPD especially over the PtAl + soot mixture. As shown in Figure 5c, the CO_x (CO_2 + CO) concentration begins to increase drastically at 350 °C during the NO_x-TPD over the

DOI: 10.1021/cs5018369
ACS Catal. 2015, 5, 909−919

soot, which is mainly ascribed to the uncatalyzed oxidation of soot by gaseous oxygen in the inlet gas. The catalytic oxidation of soot over PtZSM5 starts at a slightly lower temperature (ca. 325 °C), and the sole product is CO_2. Of particular note is that the onset of soot catalytic oxidation over PtAl is reduced to 250 °C, and the CO_2 concentration reaches the maximum at 395−425 °C. After that, the CO_2 concentration increases again and almost overlaps with that obtained from the PtZSM5 + soot mixture. The specific CO_2 product between 250 and 425 °C is supposed to be associated with the reaction between the soot and nitrate/nitrite (or their derived NO_2) on PtAl. This speculation is supported by the simultaneous decrease of the NO_2 concentration (Figure 5a) and the release of NO (Figure 5b) over PtAl + soot in this temperature range in comparison with the case for PtAl.

The so-called nitrate/nitrite-assisted soot oxidation may also occur during the soot oxidation over PtAl in NO + O_2. To find out the contribution of nitrates/nitrites in soot oxidation, the CO_x concentrations in the soot-TPO and NO_x-TPD of PtAl + soot are compared in Figure S9 (Supporting Information). The CO_x gap between these two tests can be roughly attributed to the oxidation of soot by the stored nitrates/nitrites on the catalyst. It can be seen in Figure S9 that the CO_x gap is always no more than 100 ppm, which is much smaller than the CO_x produced in soot-TPO in NO + O_2. Moreover, the amount of nitrates/nitrites adsorbed in the catalyst in NO_x-TPD (the inlet NO_2 of 500 ppm, constantly for 30 min) is much larger than the possible amount of NO_x storage during the TPO in NO + O_2 (the maximum concentration of NO_2 produced was about 400 ppm), and the contribution of nitrate/nitrite-assisted soot oxidation would be much less important in the first case. Such a phenomenon would be even more severely weakened for PtZSM5 without strong NO_x storage capacity and can thereby be excluded in this work.

3.5. In Situ DRIFTS in NO_2 + O_2. To further discuss the influence of NO_x species on soot oxidation over different catalysts, in situ FTIR experiments were recorded for PtAl and PtZSM5 with or without soot in the presence of NO_2 and O_2. The DRIFT spectra of adsorbed species on the soot-free catalyst and catalyst + soot mixtures arising in the reaction atmosphere (500 ppm of NO_2/10% O_2/N_2) were recorded, and the results are shown in Figure 6. The results obtained confirm the formation of nitrites, nitrates, and some surface oxygenated complexes on the catalyst surface. A summary of the band assignments is given in Table 4; it should be noted that the bands centered at 1360−1350 cm^{-1} can be attributed to nitrate adsorption on the CaF_2 diluent.

In the absence of soot, PtAl (Figure 6a) mainly exhibits bands corresponding to nitrates (1620 and 999 cm^{-1} for bridging nitrate; 1590, 1296, and 1035 cm^{-1} for bidentate nitrate; 1553 and 1248 cm^{-1} for monodentate nitrate) and monodentate nitrite (1495 and 1050 cm^{-1}) on alumina.[8,32,33] All of the bands assigned to nitrates remain almost unchanged with the temperature ramping from 100 to 350 °C, while a transformation of nitrites into nitrates occurred as the bands at 1495 and 1050 cm^{-1} disappeared at 300 °C.[27,28] At higher temperatures, with the decomposition of nitrates, the bands drop sharply in intensity and almost disappear at 500 °C. Over PtZSM5, nitrates (1620 and 1195 cm^{-1} for bridging nitrate; 1583 and 1296 cm^{-1} for bidentate nitrate) and monodentate nitrite species (1416 and 1150 cm^{-1}) can be observed, but they are in obviously lower intensity and are thermally unstable in comparison with the N_xO_y species on PtAl (Figure 6c).

Table 4. Band Positions and Assignments in the DRIFT Spectra of NO_2 + O_2 Adsorption

wavenumber (cm^{-1})[a]	species	ref
(1673)	gaseous NO_2	32
1620 (1620), (1195), 999	ν(N═O), $\nu_{as}(NO_2)$ and $\nu_s(NO_2)$ of bridging nitrate	8, 32, 33
1590 (1583), 1296 (1296), 1035	ν(N═O), $\nu_{as}(NO_2)$ and $\nu_s(NO_2)$ of bidentate nitrate	8, 32, 33
1553, 1248	$\nu_{as}(NO_2)$ and $\nu_s(NO_2)$ of monodentate nitrate	32
1495 (1416), 1050 (1150)	ν(N═O) and ν_{as}(N−O) of monodentate nitrite	32
1360−1350	NO_x species on CaF_2	32
[1628], [1598]	ν(N═O) of chelated and nonchelated C−NO_2	10
[1330−1300]	$\nu_s(NO_2)$ of C−NO_2 or C−N−NO_2	10, 11, 32
[1232]	ν(C−O) in C−NO_2	10, 11
[1850−1700]	ν(C═O) of carboxylic anhydrides and/or lactone	11, 12, 34
[1265−1255]	ν(C−O) of carboxylic anhydrides	11, 12, 34
[1220−1210]	ν(C−O) of lactone	8, 12
[1630−1600]	ν(C═O) of carbonyl	8, 12
[1600−1550]	ν(C═C) of quinone	8, 12

[a]The bands over PtAl, (PtZSM5), and [soot].

Furthermore, the adsorption of gaseous NO_2 can be clearly observed on PtZSM5 (1673 cm^{-1}), while it is weak on PtAl.[32] The above results agree well with the NO_x-TPD results. This reveals a stronger physical adsorption of NO_x due to the high surface area of Pt/H-ZSM5 and a weak affinity toward strong NO_x adsorption due to the high acidity of this catalyst.

Due to the strong light-absorbance properties of soot, the bands in the spectra of pure soot and the catalyst−soot mixtures exhibit much lower intensity. As shown in Figure 6e, typical N_xO_y species observed on soot are chelated and nonchelated C−NO_2 (1628 and 1598 cm^{-1}).[10] The addition of soot does not alter the adsorption bands of N_xO_y species on PtAl (Figure 6b), but it leads to blue shifts of the ν(N═O) bands of nitrates over PtZSM5 from 1620 to 1628 cm^{-1} and from 1583 to 1598 cm^{-1}, respectively (Figure 6d). The two blue-shifted adsorption bands coincide with the ν(N═O) bands of organic nitro compounds on pure soot (Figure 6e). In addition, two additional bands at 1310 and 1232 cm^{-1} assigned to $\nu_s(NO_2)$ and ν(C−O) of the C−NO_2 species are also observed on the PtZSM5 + soot mixture, which further evidences the existence of C−NO_2.[10,11] These results indicate that, over the PtZSM5 + soot mixture, NO_x prefers to adsorb on soot rather than on the catalyst.

Furthermore, in addition to the N_xO_y species, surface oxygenated complexes (SOCs) are also observed over the soot-containing samples. On pure soot, carboxylic anhydrides (1781 and 1260 cm^{-1}) are the main SOCs at 100 °C (Figure 6e), and the bands of these species increase in intensity with temperature ramping.[11,12,34] It should be noted that the bands located at 1650−1550 cm^{-1} can be assigned to carbonyl (1630 cm^{-1}) and quinone (1600 cm^{-1}) instead of nitrates at high temperatures, since no stable nitrates/nitrites exist on soot at 350 °C, as evidenced by the NO_x-TPD results.[12,29]

Different from the case of pure soot, over the PtAl + soot mixture, the anhydrides (1781 cm^{-1}) cannot be observed at temperatures lower than 150 °C. This is because PtAl may catalytically oxidize these SOCs and lead to dismissal of the corresponding band at 100 °C. However, higher temperatures result in the fast formation of anhydrides, and the

DOI: 10.1021/cs5018369
ACS Catal. 2015, 5, 909−919

decomposition rate of anhydrides could no longer match their formation rate over PtAl + soot. Furthermore, some lactone species (1765 and 1217 cm^{-1}), in addition to the anhydrides (1781 and 1255 cm^{-1}), carbonyl (1630 cm^{-1}), and quinone (1595 cm^{-1}), are also observed in a temperature range of 150−300 °C over the PtAl + soot mixture. As for the PtZSM5 + soot mixture, no SOCs are observed until the temperature reaches 250 °C, indicating good catalytic decomposition ability for the SOCs of PtZSM5, which is in agreement with the Nsoot-TPO results. Again, lactone species (1761 and 1212 cm^{-1}) are detected at 250 °C together with the anhydrides (1781 and 1265 cm^{-1}), carbonyl (1628 cm^{-1}), and quinone (1598 cm^{-1}) on PtZSM5 + soot, and the corresponding bands do not vanish with temperature ramping under the experimental conditions given.

4. DISCUSSION

4.1. NO_2 Generation and Utilization on Different Catalysts. In our experimental procedure, the soot and catalysts were mixed under the so-called loose-contact conditions, in which the NO_2 produced is a powerful and important oxidant. It has been widely accepted that the role of NO_2 is to "ignite" the soot at relatively low temperatures (e.g., <400 °C). When the temperature goes higher, excess O_2 becomes the dominant oxidant for soot oxidation.[9−12] Therefore, it is meaningful to compare the NO_x oxidation/adsorption/desorption behaviors of different catalysts and catalyst + soot mixtures to try to explore possible reaction mechanisms.

In this study, with at least 38% of the Pt inside the micropores with particle sizes smaller than 0.57 nm, the PtZSM5 catalyst exhibits an NO oxidation activity obviously lower than that of PtAl. This is considered a crucial disadvantage of PtZSM5 as a soot oxidation catalyst. However, in addition to the NO oxidation ability, the utilization of NO_2 is also critical for soot oxidation. In our previous study, the competitive adsorption of NO_x on the surface of the amphoteric and sulfated γ-Al_2O_3 supports and soot has been observed.[8] In the present work, the acidic nature of H-ZSM5 can also accelerate the transfer of the NO_2 formed on Pt active sites onto the surface of soot. Under the experimental conditions in the NO_x-TPD tests, only the physically and/or weakly adsorbed species are observed over soot, and the NO_x desorbed at high temperatures (>150 °C) comes mainly from the decomposition of stable nitrates/nitrites on the catalysts. Thus, by calculation of the NO_x desorbed at low and high temperatures separately, the amounts of NO_x adsorption on soot and stored as nitrates/nitrites over different catalysts were estimated quantitatively. On the basis of a Gaussian fitting, the deconvolution of the overlapped NO_x profiles was performed, and the data are summarized in Table 5.

As shown in Table 5, PtZSM5 exhibits a much weaker high-temperature NO_x desorption (1.33 μmol) than PtAl (6.47 μmol), proving the low NO_x storage capacity of the former catalyst. On the other hand, by subtracting the amount of low-temperature NO_x desorption over pure catalyst from that over the catalyst + soot mixture, the NO_x adsorbed on soot in different catalyst + soot mixtures were obtained. On the basis of this calculation, the amount of soot-adsorbing NO_x in the PtAl + soot mixture (0.03 μmol g_{soot}^{-1}) is negligible, indicating that the PtAl catalyst does inhibit the NO_x adsorption on soot due to the relatively strong NO_x storage capacity of the alumina support. In contrast, the amount of soot-adsorbing NO_x in the PtZSM5 + soot mixture is 0.76 μmol, which is about 1.5 times that on pure soot (0.52 μmol). These results agree well with the DRIFT spectra of NO_2 + O_2 coadsorption (Figure 6), demonstrating the preferential adsorption of NO_x on soot in the presence of the acidic PtZSM5 catalyst.

Table 5. Amounts of the NO_x Desorbed from Different Samples in the NO_x-TPD Tests

sample	low-temperature NO_x desorption (μmol)[a]	high-temperature NO_x desorption (μmol)[b]	NO_x on soot (μmol)[c]
PtAl	0.42	6.47	
PtAl + soot	0.45	5.67	0.03
PtZSM5	2.25	1.33	
PtZSM5 + soot	3.01	1.28	0.76
soot	0.52	0	0.52

[a]The amount of NO_x desorbed below 150 °C. [b]The amount of NO_x desorbed above 150 °C. [c]Calculated on the basis of the difference between the amounts of low-temperature NO_x desorption over the catalyst and the catalyst + soot mixture.

It is worth noting that, although such a "preferential adsorption" was observed in NO_x-TPD tests at temperatures much lower than those for the soot oxidation, which generally occurs above 350 °C, it still exists at mild temperature, at which the catalytic oxidation of soot occurs. Thus, it is helpful for understanding the possible involvements of NO_2 adsorption/desorption in the soot oxidation reaction. At the reaction temperatures, after production through NO oxidation over Pt, the NO_2 on PtZSM5 can hardly be stored as nitrates/nitrites due to the nature of the acidic support. NO_2 may thus spill onto the soot surface, first physically and/or weakly adsorbing on soot, and then rapidly react with soot to generate SOCs. This speculation was further proved by the in situ DRIFTS results. As shown in Figure 6d, the adsorption bands at 1330−1300 cm^{-1} (centered at 1312 cm^{-1}) and 1232 cm^{-1} attributed to $\nu_s(NO_2)$ and ν(C−O) of the C−NO_2 species can be clearly observed on the PtZSM5 + soot mixture at temperatures below 200 °C. At higher temperatures (>200 °C), these species will transform into SOCs once formed and thereby cannot be observed.[11] On the other hand, the absence of these IR bands over pure soot (Figure 6e) should be ascribed to the lack of intense C−NO_2 reactions without catalyst, which produce much less nitro compounds.

4.2. Effects of PtZSM5 on SOCs Formation and Decomposition. In view of the soot oxidation mechanism, the process should involve the formation and decomposition of surface oxygenated complexes.[8,35] The first step has been widely accepted to mainly occur via C−NO_2 reactions, and the latter may involve the oxidation of SOCs by both NO_2 and O_2.[8,12,35] In this study, these two steps are both likely to be accelerated over the PtZSM5 catalyst.

As shown in section 3.2, a promotion effect of PtZSM5 on the decomposition of SOCs is verified by the comparison of the catalytic oxidation of Nsoot (with abundant SOCs on the surface) and soot in O_2. This promotion effect also exists in the presence of NO_x. There are four types of SOCs that are detected over soot in the DRIFT spectra obtained in NO_2/O_2, which are lactone (190−650 °C, thermal decomposition temperature, similarly hereinafter), carboxylic anhydrides (350−627 °C), carbonyl (700−980 °C), and quinone (700−980 °C).[11] Since the spectra of the last two species are overlapped with those of the nitrates/nitrites, the following

DOI: 10.1021/cs5018369
ACS Catal. 2015, 5, 909−919

discussion is focused on the former two species. As shown in Figure 6e, some carboxylic anhydrides are observed on the surface of pure soot at a temperature as low as 100 °C. Meanwhile, the bands of carboxylic anhydrides and lactone appear on PtAl + soot at a slightly higher temperature (150 °C, Figure 6b). These species cannot be observed on the PtZSM5 + soot mixture until the temperature increases to 250 °C (Figure 6d). Since the formation and decomposition of SOCs occur simultaneously, the absence of SOCs bands may be attributed either to an inhibited SOCs formation or to a decomposition rate faster than the formation of these SOCs species. As presented in section 4.1, there should be more chances for C−NO_2 reactions due to the promoted transfer of NO_2 from the acidic PtZSM5 onto the soot surface, and the formation of SOCs can also be promoted theoretically. Thus, it is reasonable to suggest that, although the formation of SOCs was accelerated, their catalytic decomposition rate is even higher over PtZSM5 at temperatures below 250 °C.

The mechanism of acceleration on SOCs decomposition over PtZSM5 cannot yet be clearly clarified without strong experimental evidence. However, it may be explained by an acid-assisted mechanism, in which the role of strong acid sites is to produce the carbon radical cation intermediates, which are highly active and can be easily oxidized.[19,25,36−38] This process can be achieved either by electron transfer involving Lewis acid sites or by hydroxylation−deprotonation involving Brønsted acid sites. Such an electronic interaction between catalysts and soot is possible even under "loose" catalyst−soot contact conditions, as proposed by Oi-Uchisawa et al.[6] With the synergistic effect of strong acid sites and surface Pt, PtZSM5 catalyst exhibits a superior acceleration on SOCs decomposition. To further confirm this speculation, different Pt/zeolite catalysts were synthesized, and a good agreement in the acceleration of SOCs decomposition (expressed in the form of $r_{Nsoot} - r_{soot}$) and the amount of surface strong acid sites over different catalysts can be observed (Figure S10, Supporting Information).

It is worth noting that the SOCs decomposition ability should not be taken as the sole factor that influences the catalysts' soot oxidation activity. As shown in Table 2, with strong acid sites on the surface, ZSM5 can partially promote the decomposition of SOCs on Nsoot. However, its reaction rate is still much lower than that on PtAl. This is because, once the SOCs on the outer layer of Nsoot decomposed, H-ZSM5 alone lacks the strong ability to generate them again. In this sense, the formation of SOCs is also crucial to the catalytic oxidation of soot. The promoted formation of SOCs over PtZSM5 can be verified by the DRIFT results. Lactone is a thermally unstable species in comparison with the other three SOCs. It is not observed on pure soot (Figure 6e) due to the rapid oxidation by NO_2 to CO_x or other relatively thermally stable species. However, this species is observed in the spectra of the catalyst + soot mixtures, which is due to the faster formation rate catalyzed by the catalysts. It is importantly found that lactone is observed on PtAl + soot at temperatures no higher than 300 °C, and it still exists on PtZSM5 + soot even at 550 °C. This implies that PtZSM5 leads to a fast formation of lactone, and the decomposition of these species no longer match their formation rate.

Consequently, the promoting effects on both formation and decomposition of SOCs exist on PtZSM5. Both the preferential adsorption of NO_2 and the electronic interactions between soot and the strong acid sites over PtZSM5 may play important roles in the reactions. These should be the so-called "improvement" in section 3.1 that counteracted the negative influence of the weakened NO oxidation activity of PtZSM5, which makes PtZSM5 exhibit a higher catalytic activity for soot oxidation than PtAl. Nevertheless, the aforementioned acid-assisted mechanism requires more strong experimental evidence such as in situ EPR studies to be certified and improved in the future.[19]

5. CONCLUSIONS

In this study, due to at least 38% of the Pt inside micropores of H-ZSM5 support with small particle size (≤0.57 nm), the Pt/H-ZSM5 catalyst exhibits a lower NO oxidation activity in comparison with the commercial Pt/Al_2O_3 catalyst. After exclusion of the influences of surface Pt particle size distributions and initial Pt oxidation states, however, Pt/H-ZSM5 exhibits obviously higher soot oxidation activities than Pt/Al_2O_3. In the presence of NO_x, the acidic H-ZSM5 support promotes the preferential adsorption of NO_2 on the surface of soot, providing more chances for NO_2−soot reactions. In addition to the efficient utilization of NO_2, the in situ DRIFT and Nsoot-TPO results reveal that, with the synergistic effect of surface Pt, the surface strong acid sites may catalyze the formation and decomposition of surface oxygenated complexes (SOCs) on soot. Thus, both NO_2- and acid-assisted soot oxidation mechanisms contribute to the high activity of Pt/H-ZSM5 catalyst.

■ ASSOCIATED CONTENT

Supporting Information

The following file is available free of charge on the ACS Publications website at DOI: 10.1021/cs5018369.

Calculation process of surface Pt content based on CO titration and HRTEM data, calculation process of TOF_{Pt}, and Figures S1−S9 (PDF)

■ AUTHOR INFORMATION

Corresponding Authors

*E-mail for X.W.: wuxiaodong@tsinghua.edu.cn.

*E-mail for D.W.: duanweng@tsinghua.edu.cn.

Notes

The authors declare no competing financial interest.

■ ACKNOWLEDGMENTS

The authors acknowledge Project 2013AA061902 by the Ministry of Science and Technology of China and Project 113007A by the Ministry of Education of China. We also acknowledge financial support from the Key Laboratory of Advanced Materials of Ministry of Education.

■ REFERENCES

(1) Aneggi, E.; Wiater, D.; Leitenburg, C.; Llorca, J.; Trovarelli, A. *ACS Catal.* **2014**, *4*, 172−181.

(2) Yamazaki, K.; Kayama, T.; Dong, F.; Shinjoh, H. *J. Catal.* **2011**, *282*, 289−298.

(3) Villani, K.; Vermandel, W.; Smets, K.; Liang, D. D.; Tendeloo, G. V.; Martens, J. A. *Environ. Sci. Technol.* **2006**, *40*, 2727−2733.

(4) Wei, Y. C.; Liu, J.; Zhao, Z.; Xu, C. M.; Duan, A. J.; Jiang, G. Y. *Appl. Catal., A* **2013**, *453*, 250−261.

(5) Oi-Uchisawa, J.; Obuchi, A.; Enomoto, R.; Liu, S. T.; Nanba, T.; Kushiyama, S. *Appl. Catal., B* **2000**, *26*, 17−24.

(6) Oi-Uchisawa, J.; Obuchi, A.; Ogata, A.; Enomoto, R.; Kushiyama, S. *Appl. Catal., B* **1999**, *21*, 9−17.

DOI: 10.1021/cs5018369
ACS Catal. 2015, 5, 909−919

(7) Oi-Uchisawa, J.; Obuchi, A.; Enomoto, R.; Xu, J. Y.; Nanba, T.; Liu, S. T.; Kushiyama, S. *Appl. Catal., B* **2001**, *32*, 257−268.
(8) Liu, S.; Wu, X. D.; Weng, D.; Li, M.; Fan, J. *Appl. Catal., B* **2013**, *138*−*139*, 199−211.
(9) Jeguirim, M.; Tschamber, V.; Brilhac, J. F.; Ehrburger, P. *Fuel* **2005**, *84*, 1949−1956.
(10) Muckenhuber, H.; Grothe, H. *Carbon* **2007**, *45*, 321−329.
(11) Muckenhuber, H.; Grothe, H. *Carbon* **2006**, *44*, 546−559.
(12) Setiabudi, A.; Makkee, M.; Moulijn, J. A. *Appl. Catal., B* **2004**, *50*, 185−194.
(13) Bahrami, B.; Komvokis, V. G.; Singh, U. G.; Ziebarth, M. S.; Alexeev, O. S.; Amiridis, M. D. *Appl. Catal., A* **2011**, *391*, 11−21.
(14) Aranzabal, A.; González-Marcos, J. A.; Romero-Sáez, M.; González-Velasco, J. R.; Guillemot, M.; Magnoux, P. *Appl. Catal., B* **2009**, *88*, 533−541.
(15) Jin, H. L.; Ansari, M. B.; Jeong, E.; Park, S. *J. Catal.* **2012**, *291*, 55−62.
(16) Aboul-Gheit, A. K.; Aboul-Fotouh, S. M. *J. Taiwan Inst. Chem. Eng.* **2012**, *43*, 711−717.
(17) Scirè, S.; Minicò, M.; Crisafulli, C. *Appl. Catal., B* **2003**, *45*, 117−125.
(18) Wang, A. Q.; Ma, L.; Cong, Y.; Zhang, T.; Liang, D. B. *Appl. Catal., B* **2003**, *40*, 319−329.
(19) Corma, A.; García, H. *Chem. Rev.* **2002**, *102*, 3837−3892.
(20) Liu, J.; Zhao, Z.; Xu, C. M.; Duan, A. J.; Jiang, G. Y. *Energy Fuels* **2010**, *24*, 3778−3783.
(21) Corro, G.; Cano, C.; Fierro, J. L. G. *J. Mol. Catal. A: Chem.* **2010**, *315*, 35−42.
(22) Smeltz, A. D.; Delgass, W. N.; Ribeiro, F. H. *Langmuir* **2010**, *26*, 16578−16588.
(23) Lira, E.; Merte, L. R.; Behafarid, F.; Ono, L. K.; Zhang, L.; Cuenya, B. R. *ACS Catal.* **2014**, *4*, 1875−1884.
(24) Xue, Z. T.; Zhang, T.; Ma, J. H.; Miao, H. X.; Fan, W. M.; Zhang, Y. Y.; Li, R. F. *Microporous Mesoporous Mater.* **2012**, *151*, 271−276.
(25) Ungureanu, A.; Hoang, T. V.; Trong On, D.; Dumitriu, E.; Kaliaguine, S. *Appl. Catal., A* **2005**, *294*, 92−105.
(26) Zhu, Z. P.; Liu, Z. Y.; Liu, S. J.; Niu, H. X. *Fuel* **2000**, *79*, 651−658.
(27) Azambre, B.; Atribak, I.; Bueno-López, A.; García-García, A. *J. Phys. Chem. C* **2010**, *114*, 13300−13312.
(28) Atribak, I.; Azambre, B.; Bueno-López, A.; García-García, A. *Appl. Catal., B* **2009**, *92*, 126−137.
(29) Sánchez, B. S.; Querini, C. A.; Miró, E. E. *Appl. Catal., A* **2009**, *366*, 166−175.
(30) Artioli, N.; Matarrese, R.; Castoldi, L.; Lietti, L.; Forzatti, P. *Catal. Today* **2011**, *166*, 36−44.
(31) Klein, J.; Fechete, I.; Bresset, V.; Garin, F.; Tschamber, V. *Catal. Today* **2012**, *189*, 60−64.
(32) Hadjiivanov, K. I. *Catal. Rev. Sci. Eng.* **2000**, *42*, 71−144.
(33) Toops, T. J.; Smith, D. B.; Partridge, W. P. *Appl. Catal., B* **2005**, *58*, 245−254.
(34) Kantcheva, M.; Ciftlikli, E. Z. *J. Phys. Chem. B* **2002**, *106*, 3941−3949.
(35) Setiabudi, A.; Chen, J. L.; Mul, G.; Makkee, M.; Moulijn, J. A. *Appl. Catal., B* **2004**, *51*, 9−19.
(36) Khenkin, A. M.; Weiner, L.; Wang, Y.; Neumann, R. *J. Am. Chem. Soc.* **2001**, *123*, 8531−8542.
(37) Guisnet, M.; Dégé, P.; Magnoux, P. *Appl. Catal., B* **1999**, *20*, 1−13.
(38) Sheldon, R. A.; Kochi, J. K. *Metal Catalyzed Oxidation of Orgainic Compounds*; Academic Press: New York, 1981.

DOI: 10.1021/cs5018369
ACS Catal. 2015, 5, 909−919